Applied Catalysis B: Environmental 88 (2009) 25–31

Contents lists available at ScienceDirect

Applied Catalysis B: Environmental

journal homepage: www.elsevier.com/locate/apcatb

Adsorption/desorption of dimethylsulfide on activated carbon modified with iron chloride

Hong Cui, Scott Q. Turn *

Hawaii Natural Energy Institute, University of Hawaii at Manoa, 1680 East–West Road, Post 109, Honolulu, HI 96822, United States

ARTICLE INFO

Article history:
Received 19 June 2008
Received in revised form 19 September 2008
Accepted 24 September 2008
Available online 8 October 2008

Keywords:
Activated carbon
Adsorption
Temperature programmed desorption
Dimethylsulfide
Iron chloride

ABSTRACT

The adsorption capacity of activated carbon for the natural gas contaminant dimethylsulfide (DMS) was improved by impregnating it with $FeCl_3$ introduced in solution to affect surface modification. A DMS adsorption mechanism and roles of impregnated $FeCl_3$ on the capacity enhancement were proposed based on experimental tests results.

Samples of activated carbon and activated carbon impregnated with $FeCl_3$ were tested as DMS sorbents. Samples loaded with DMS were subsequently extracted with *n*-octane and the resulting solvents were analyzed for sulfur species using a gas chromatograph equipped with a sulfur chemiluminescence detector. No other sulfur compounds were detected in the liquid samples other than DMS. DMS, dimethyl disulfide, and carbonyl sulfide were recovered from identical DMS-adsorbed samples of activated carbon impregnated with $FeCl_3$ subjected to temperature programmed desorption (TPD) in a nitrogen gas stream. Only DMS was recovered from the activated carbon samples. The TPD patterns indicate different kinetics of DMS desorption related to the carbon phase and the new active sites created by the $FeCl_3$ impregnation. The new active sites improved DMS adsorption capacity and likely had stronger affinity with DMS molecule. As a reference, similar tests were investigated using methyl mercaptan (MM) as an adsorbate on the carbon sorbents. A different adsorption mechanism was found and discussed from these experimental results. Regeneration of the used carbon sorbents by thermal desorption was also explored.

© 2008 Elsevier B.V. All rights reserved.

1. Introduction

Dimethylsulfide (DMS) is a non-polar, stable, organic, reduced sulfur compound present in the natural environment. It is the dominant sulfur compound in seawater [1,2] and is also produced in industrial processes. DMS can be used as an ingredient in odorants for pipeline gas due to its stable chemical characteristics even when exposed to black iron pipes and tanks [1]. Sulfur odorants are added to pipeline gas as a safety precaution but must be completely removed if the pipeline gas is to be used as a feedstock for H_2 production to supply fuel cells. Thus sulfur removal is an important step in fuel processing.

One method for sulfur odorant removal from pipeline gas is adsorption using activated carbon [1,3–16]. Modification of carbon surfaces by using either oxidation or impregnation has been explored as a method to improve sulfur adsorption capacity and consequently reduce the sorbent consumption. Greater sulfur capacity results from the creation of more functional groups or active adsorption sites on the carbon surface. Adsorptive sites may oxidize reduced sulfur molecules, creating bigger molecules which are more easily adsorbed in the micropores of activated carbon. An example of this is the improvement of methyl mercaptan (MM) adsorptive capacity by carbon surface modification. Oxygen functional groups facilitate the oxidation of MM to form dimethyl disulfide (DMDS) [8,13]. DMDS is a larger molecule with a higher boiling point and is more easily adsorbed in the carbon micropores.

Similar efforts have been attempted to remove DMS, which is regarded as the most difficult sulfur compound [5,12,17,18] to remove from pipeline gas by adsorption. Oxidation/adsorption is one applicable path for DMS occupancy on the carbon surface and the activated carbon surface can be modified to enhance its sulfur capacity. In a previous investigation using pipelined synthetic natural gas (SNG) [17,18], activated carbon modified with iron chloride ($FeCl_3$) solution had a slightly greater DMS adsorptive capacity (0.03 mg S g^{-1} carbon) compared with the 12 other virgin and modified carbons that displayed almost zero capacity. The role of $FeCl_3$ on oxidation/adsorption has been pointed out in the case of MM [19], which was assumed to be oxidized to DMDS by the catalytic participation of iron on the carbon surface. For DMS adsorption, however, no such investigations were found in the literature. Efforts

* Corresponding author.
E-mail address: sturn@hawaii.edu (S.Q. Turn).

0926-3373/$ – see front matter © 2008 Elsevier B.V. All rights reserved.
doi:10.1016/j.apcatb.2008.09.025

to improve the adsorptive capacity of activated carbon for DMS by means of surface modification would benefit from a better understanding of the adsorption behavior and mechanism.

An objective of this paper is to investigate the adsorption behavior and mechanism of DMS on activated carbon sorbent that was modified with $FeCl_3$. This effort was based on the analysis of sulfur species removed from sorbent loaded with DMS using mild extraction with solvent and temperature programmed desorption (TPD). As a reference, similar tests were conducted to investigate MM adsorption/desorption behaviors using the same carbon sorbents. Experimental results could verify if the oxidation/adsorption mechanism can be applied to MM and DMS adsorption on the modified carbons.

2. Experimental

2.1. Sorbents preparation and properties

A coconut shell activated carbon (OLC Plus 12 × 30, Calgon Carbon Corporation) was used as the parent carbon in this study. $FeCl_3$ was loaded using an impregnation method to produce a concentration of 0.4 mmol metal (Fe^{3+}) per gram carbon. Details of the impregnation process can be found elsewhere [18,20].

The basic pore properties for the original and modified carbon sorbents are presented in Table 1. Nitrogen (liquid N_2) adsorption/desorption isotherms for the samples were measured at 77 K (Autosorb®-1, Quantachrome Instruments, Boynton Beach, FL). Before the measurements, samples were heated and degassed at 110 °C for 2 h under a vacuum of 10^{-5} torr (1.33×10^{-7} Pa). Specific surface area (S_{BET}) was calculated by using the multipoint BET method in the relative pressure (P/P_0) range of 0.01–0.1. The total pore volume (V_0) and the average pore diameter (D_{ave}) were calculated from the amount of gas adsorbed at the related pressure of 0.995–0.999. In addition, density functional theory (DFT) was used to analyze the pore structure parameters, including micropore volume (V_{micro} – pore width less than 2 nm), total pore volume (V_{total} – pore width less than 36 nm), and mode pore width (D_w). The DFT calculation method is provided from the Autosorb®-1 data processing software and assumes that the activated carbon contains slit-shaped pores.

2.2. Experimental apparatus and analysis process

The laboratory scale apparatus consisting of a sulfur gas generator, sorbent column, and sulfur detector, is shown in Fig. 1. The trace gas generator (Model CO395, Kin-Tek Laboratories, La Marque, TX) loaded with a DMS permeation tube (KIN-TEK Part No. HRT-006.50-1006/40) served as a sulfur source. Permeation tubes provide a calibrated mass emission rate at constant temperature under an inert purge flow. A DMS emission rate of 1268 ng min^{-1} at 40 °C was combined with an N_2 carrier gas flow to provide a gas with regulated DMS concentration. A permeation tube (KIN-TEK Part No. SRT-2-010.00-1004/50) with an emission rate of 1015 ng MM min^{-1} at 50 °C was used for the MM tests.

A 35 ml glass pipette was used as a sorbent column. The column was oriented vertically for adsorption and extraction tests, and was placed in a tube furnace horizontally for TPD tests. Two types of adsorption tests were performed. The first type included breakthrough and TPD tests, using 0.2 g sorbent samples. The sulfur capacity (milligram S per gram activated carbon) was also determined from these tests. The second type was quantitative adsorption tests, in which 1.5 g carbon sorbent was subjected to adsorption of DMS for 15 to 16 h without experiencing break through. The resulting samples contained a known mass of S and

Table 1
Properties of activated carbon sorbents.

Sample name	S_{BET} (m^2/g) (P/P_0 = 0.01–0.1)	V_0 (cm^3/g) (P/P_0 = 0.995–0.999)	D_{ave} (nm)	Pore structure parameter by DFT calculation		
				V_{micro} (cm^3) (less than 2 nm)	V_{total} (cm^3) (less than 36 nm)	D_w (nm) (mode)
AC	1252.9	0.601	0.960	0.450	0.538	0.600
AC–$FeCl_3$	864.4	0.481	0.223	0.306	0.422	0.786

S_{BET} – specific surface area; V_0 – total pore volume; D_{ave} – average pore diameter; V_{micro} – pore width less than 2 nm; V_{total} – pore width less than 36 nm; D_w – mode pore width; DFT – density functional theory.

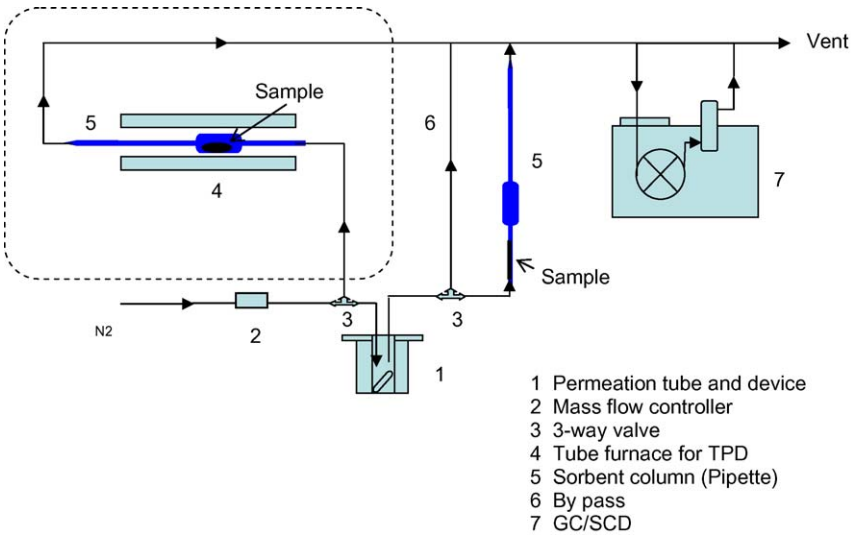

Fig. 1. Experimental setup for carbon sorbents adsorption and desorption.

were used in subsequent extraction and TPD tests to allow S mass balances to be performed. During both types of adsorption tests, the DMS permeation tube device was used to generate a N_2 stream containing 1.40 ppm DMS at a flow rate of 326 ± 2 ml min^{-1}. Both types of adsorption tests were conducted at ambient conditions (typically 26 °C and 0.1 MPa).

After the adsorption tests were completed, sorbents loaded with DMS were extracted with *n*-octane. A 0.2 g sorbent sample loaded with DMS from the quantitative adsorption tests was packed into a vertically-positioned pipette. Each sample was leached three times with 10 ml of *n*-octane. The resulting 30 ml solvent volume was analyzed for sulfur compounds. This was a mild extraction process that was not expected to extract all adsorbed compounds from the sorbents and the solid sample in the pipette was subsequently subjected to TPD testing. In addition, 0.2 g samples of non-extracted sorbents from the same quantitative adsorption tests were subjected to TPD testing. The sample temperature was ramped from 25 °C to 300 °C at 1 °C min^{-1} using a programmable tube furnace. N_2 was used as a sweep gas at a flow of 326 ± 2 ml min^{-1} and the exit gas was analyzed for sulfur compounds.

Gaseous samples were analyzed for sulfur using a Shimadzu 2014 gas chromatograph (GC) equipped with a capillary column (Rtx-1, 60m-0.53-7um, Restek Corporation) and sulfur chemiluminescence detector (SCD) (Sievers Model 355, GE Analytical Instruments, Boulder, CO). Helium served as the carrier gas and a six-port sampling valve equipped with a 125 μl sample loop was used to make automatic injections. In each analysis the column temperature was held for 1 min at 50 °C, ramped to 125 °C at 20 °C min^{-1}, ramped a second time to 180 °C at 10 °C min^{-1}, held at 180 °C for 1 min, and finally cooled to 50 °C at 100 °C min^{-1}. Thus, effluent gas was able to be sampled and analyzed with a cycle time of 15 min. In addition, DMS was analyzed from a bypass path before and after the adsorption and desorption tests, to make calibrations and to confirm that the system was operating stably.

Sulfur analyses of the liquid samples were performed by manual injection on the same GC using an injection volume of 2 μl. Because the sulfur SCD produces an equimolar response to sulfur, independent of the host sulfur compound, 25 ppm (±0.5%) H_2S calibration gas (Scotty® 58, Scott Specialty Gases) was used in the sulfur analysis for the liquid samples. Other analytical parameters were the same used for the gas samples.

The test procedures outlined above for DMS were used for the MM tests as well.

3. Results and discussion

3.1. Breakthrough curves

The adsorption of DMS (1.40 ppm) in an N_2 carrier gas on activated carbon sorbents was carried out to estimate sulfur capacities and evaluate sulfur capture capabilities. Fig. 2 shows the breakthrough curves of virgin carbon (AC) and carbon loaded with $FeCl_3$ (AC–$FeCl_3$). The adsorptive capacities of the two carbon sorbents are also shown in this figure; 3.32 mg S g^{-1} sorbent for AC–$FeCl_3$ and 2.23 mg S g^{-1} sorbent for AC. The adsorption capacity was calculated by integrating the area under the DMS breakthrough curve and subtracting it from the total sulfur input up to the point of breakthrough. The breakthrough time is defined as the point at which the DMS concentration in the effluent gas reached 0.2 ppm. Obviously, the impregnation of $FeCl_3$ leads to increases in the breakthrough time and in the amount of DMS adsorbed by the carbon, despite a notable decrease in the surface area, micropore area, and volume (data shown in Table 1). Both samples primarily possess micropores that are less than 2 nm in width and the impregnation of $FeCl_3$ did not change the pore size distribution to a great extent. Complete analysis of sample pore size distributions have been report elsewhere [20]. From this it can be inferred that the significant factor in the improvement of DMS capacity results from the new chemical properties produced by the addition of $FeCl_3$, rather than changes in the physical properties such as pore surface area and pore structure of carbon phase.

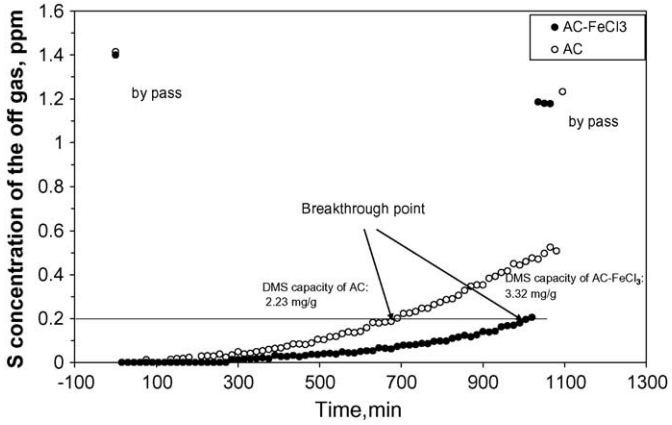

Fig. 2. DMS breakthrough curves for activated carbon (AC) and activated carbon impregnated with $FeCl_3$ (AC–$FeCl_3$).

Adsorption of MM (1.43 ppm in N_2) on AC and AC–$FeCl_3$ was also carried out. Breakthrough was not observed for either of the sorbents during the test time up to 20 h, indicating that MM is more easily captured by the carbon sorbents than DMS.

3.2. Extraction analysis

If the oxidation/adsorption reaction occurs on the carbon surface, then it would be expected that the oxidation products could be dissolved and recovered by solvent extraction and that sulfur compounds could be identified by analysis of the solvent. The properties of possible oxidation products with their precursor are listed in Table 2.

Table 2
Basic properties of sulfur compounds of interest.

	Chemical name				
	MM	DMDS	DMS	DMSO	DMSO2
Molecular formula	$H_3C–SH$	$H_3C–S=S–CH_3$	$H_3C–S–CH_3$	$H_3C-\overset{\overset{O}{\|}}{S}-CH_3$	$H_3C-\overset{\overset{O}{\|}}{\underset{\underset{O}{\|}}{S}}-CH_3$
Molar mass (g/mol)	48.11	94.19	62.13	78.13	94.13
Density (g/cm^3)	–	1.06	0.840	1.100	–
Melting point (°C)	−123	−85	−98	18.5	109
Boiling point (°C)	5.95	109	37	189	238

The MM adsorption and oxidation to DMDS is described by three global reactions steps, equations (1)–(3). MM is adsorbed onto the activated carbon surface and then oxidized by the oxidation functional groups or adsorbed oxygen. The product DMDS is adsorbed more strongly than MM due to its larger size and higher boiling point. Metal impurities (such as $FeCl_3$) could play important roles in catalytic oxidation, since metal impurities can transfer oxygen to the adsorbed MM. A more detailed discussion of MM adsorption mechanism can be found elsewhere [21].

$$CH_3SH_g \rightarrow CH_3SH_{ads} \quad (1)$$

$$O_{2ads} \rightarrow 2O_{ads} \quad (2)$$

$$2CH_3SH_{ads} + O_{ads} \rightarrow CH_3SSCH_{3ads} + H_2O \quad (3)$$

Fig. 3 shows the sulfur speciation results by GC/SCD analysis of the extract samples resulting from *n*-octane leaching of AC and AC–$FeCl_3$ quantitatively loaded with MM. DMDS was detected as the single peak in the chromatogram indicating that DMDS was formed on the carbon surface during MM adsorption process. AC and AC–$FeCl_3$ were equally capable of converting MM to DMDS at these test conditions, as no other sulfur compounds were observed in the extracts. Recall that MM breakthrough was not obtained for AC or AC–$FeCl_3$ over a 20 h test period. Likewise the current data does not reveal distinct difference between the two sorbents and does not illuminate the role of impregnated $FeCl_3$ on the MM oxidation/adsorption process. It is reasonable to believe, however, that $FeCl_3$ is an oxidant that can provide or create more active sites for sulfur compounds on the carbon surface. These adsorption sites perhaps are functional groups containing oxygen, metal anions (Fe^{3+}), or chlorine with negatively-charged ions (Cl^-).

It is noted that the molecular structures of DMS and MM are different. DMS molecule does not have the polar group (–SH) that MM does and it includes two pairs of lone electrons around the S atom. This gives a higher nucleophilicity that could be attacked by an electrophile. The possible oxidation products would be dimethyl sulfoxide (DMSO) by the attack of one oxygen atom, or dimethyl sulfone (DMSO2) by the attack of two oxygen atoms. These oxidation products have bigger molecular sizes and considerably higher boiling points as shown in Table 2 and could be easier to adsorb in micropores of activated carbons. A possible path for the oxidation/adsorption process is shown in equation (4).

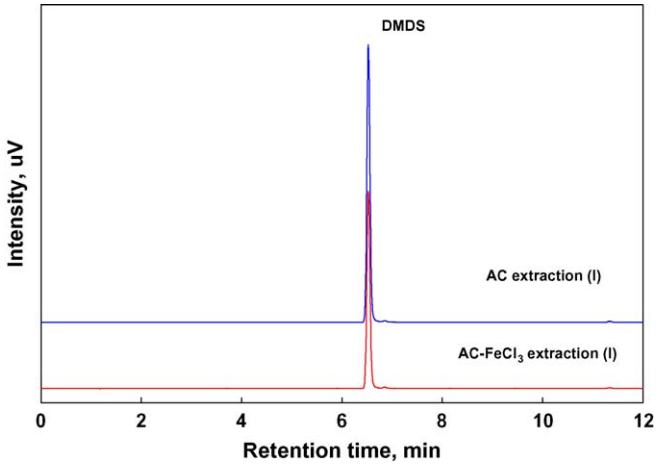

Fig. 3. Chromatograms of sulfur species in *n*-octane-extract of AC and AC–$FeCl_3$ adsorbed with MM.

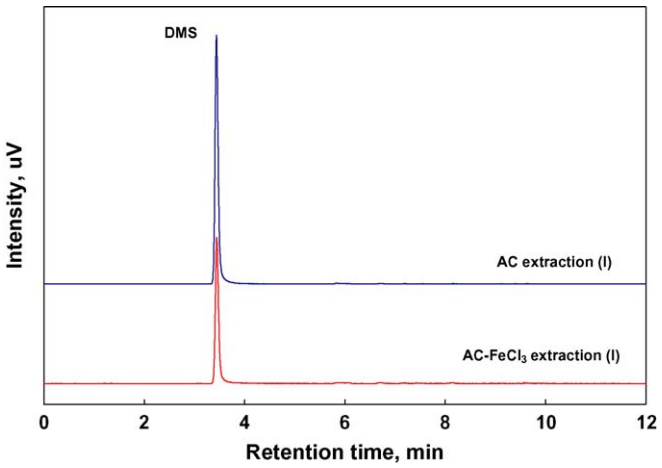

Fig. 4. Chromatograms of sulfur species in *n*-octane-extract of AC and AC–$FeCl_3$ adsorbed with DMS.

$$H_3C{-}S{-}CH_3 \rightarrow H_3C{-}\overset{\overset{O}{\|}}{S}{-}CH_3 \rightarrow H_3C{-}\overset{\overset{O}{\|}}{\underset{\underset{O}{\|}}{S}}{-}CH_3 \quad (4)$$

Fig. 4 shows the sulfur speciation results by GC/SCD analysis of the extract samples resulting from *n*-octane leaching of AC and AC–$FeCl_3$ quantitatively loaded with DMS. DMS was detected as the

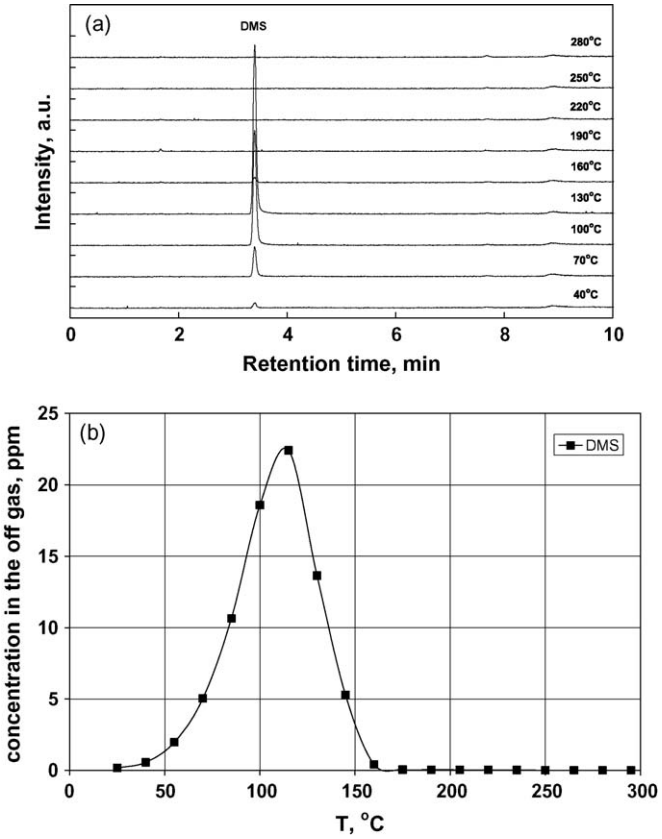

Fig. 5. GC SCD chromatograms (a) and associated TPD profiles (b) from analyses of the N_2 sweep gas at the exit of the test apparatus during thermal desorption of the AC samples with DMS adsorbed.

single peak in the GC profiles, and no other sulfur compounds were observed in either of the extracts. This indicates that DMS is the only extractable compound occupying the carbon surfaces of both AC and AC–$FeCl_3$. It also suggests that adsorption plays an important role in the increased DMS capacity displayed by AC–$FeCl_3$ (Fig. 1) rather than adsorption/oxidation of DMS on the carbon surface. Unlike methyl mercaptan that has both polar (–SH) and non-polar ($–CH_3$) functional groups, DMS lacks the polar group (–SH) that would result in strong affinity towards other polar functional groups on the carbon surface.

3.3. Temperature programmed desorption (TPD)

An adsorption/oxidation mechanism cannot explain the increased DMS capacity of AC–$FeCl_3$, since no sulfur compounds other than DMS were detected in the extract samples. TPD was used to gain insight into the role of $FeCl_3$ in the improvement of DMS capacity and the possible adsorption mechanism for DMS on the carbon surface.

Figs. 5(a) and 6(a) show GC SCD chromatograms from analyses of the N_2 sweep gas at the exit of the apparatus for TPD tests of sorbents AC and AC–$FeCl_3$, respectively, that had been previously used in DMS adsorption tests. The relationships of sulfur compound concentrations in the off gas to desorption temperatures are presented in Figs. 5(b) and 6(b).

As shown in Fig. 5, only DMS was found to be released in the TPD test of sorbent AC. DMS was first detected at room temperature (25 °C), reached a maximum at ~115 °C, and completed desorption at ~160 °C. DMS, COS, and DMDS were detected in the effluent gas generated from AC–$FeCl_3$ during the TPD process as shown in Fig. 6. The desorption of DMS has a bimodal relationship to temperature with maxima at 85 °C and 175 °C. At temperatures above 120 °C, COS and DMDS were also detected in the effluent gas, accompanying DMS.

Comparing Figs. 5(b) and 6(b) shows that the first DMS release peak for AC–$FeCl_3$ has the same temperature range observed for AC. This peak reflects a weak interaction of DMS with the carbon phase. The second DMS peak appeared at higher temperature and was only observed for AC–$FeCl_3$ indicating that $FeCl_3$ provides new adsorption sites on the modified carbon surface. The higher release temperature reflects a stronger interaction between the DMS molecules and these new adsorption sites.

The bimodal desorption peaks are not found in the TPD profiles shown in Fig. 7(a) and (b) for sorbents AC and AC–$FeCl_3$ with MM adsorbed. DMDS was a primary sulfur compound detected at the exit of TPD processes for both AC and AC–$FeCl_3$ and no MM was detected. This verifies that adsorption/oxidization of MM occurs on the carbon surface and the resulting oxidization product is DMDS. Moreover, a single TPD peak of DMDS indicates that $FeCl_3$ does not provide another adsorptive position for DMDS on the carbon surface. If it did, multiple peaks indicating different adsorption paths would be detected.

It should be noted that DMDS and COS were also found in the TPD processes for AC–$FeCl_3$ loaded with DMS, but were not found in its extract sample, as shown in Figs. 4 and 6. These sulfur compounds are regarded as the interaction products of DMS and surface C–O complexes generated during TPD at elevated temperatures with the catalysis of $FeCl_3$. Similarly, COS is also found in the TPD process gas produced from AC and AC–$FeCl_3$ adsorbed with MM. Greater amounts of COS were released from

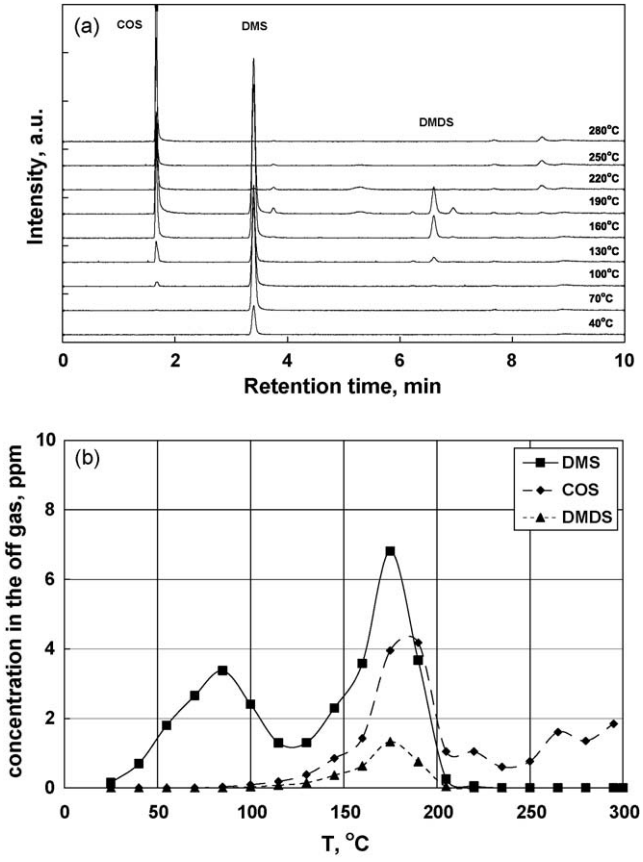

Fig. 6. GC SCD chromatograms (a) and associated TPD profiles (b) from analyses of the N_2 sweep gas at the exit of the test apparatus during thermal desorption of the AC–$FeCl_3$ samples with DMS adsorbed.

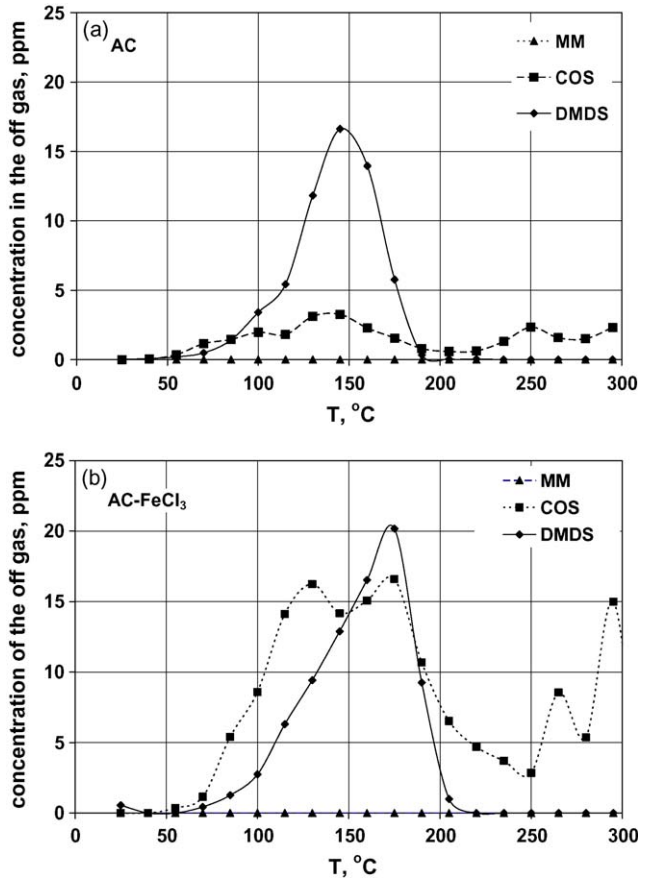

Fig. 7. TPD profiles during thermal desorption of AC (a) and AC–$FeCl_3$(b) with MM adsorption.

the AC–$FeCl_3$ test, indicating that $FeCl_3$ may serve as a catalyst in the decomposition reaction. The detailed reaction path needs to be explored further.

3.4. Thermal regeneration and mass balance

Thermal desorption was considered as an option for spent sorbent regeneration. Fig. 8(a) shows the DMS breakthrough behavior for virgin AC sorbent and for AC sorbent that had been used in a DMS breakthrough test with subsequent TPD regeneration (sample identified as AC-R1). After the breakthrough test of Fig. 8(a), samples AC and AC-R1 was subjected to TPD regeneration and the results are compared in Fig. 8(b). Similarly, the adsorption and TPD behaviors of sorbent AC–$FeCl_3$ and the regenerated samples (AC–$FeCl_3$-R1, R2 and R3) are shown in Fig. 9.

Compared with original AC, the adsorption/desorption behaviors of spent sorbent (AC-R1) are very similar. This indicates that heating to 300 °C in an inert atmosphere had no impact on AC's adsorptive ability and the spent AC could be regenerated by thermal desorption without capacity loss. This is not the case for AC–$FeCl_3$ where the spent samples display a shorter breakthrough time than the original AC–$FeCl_3$. The regenerated samples displayed similar adsorption and TPD trends through three adsorption-desorption cycles and were similar to that of the virgin carbon sample, AC. This shows that the new adsorption sites created by $FeCl_3$ modification on the carbon surface are not thermally stable and could not be regenerated by thermal desorption.

The AC and AC–$FeCl_3$ samples that were extracted by *n*-octane were also subjected to TPD tests. The TPD profiles of DMS release are shown in Fig. 10. Compared with the TPD patterns of samples that were not extracted (Figs. 5 and 6), the DMS release peaks shift to lower temperatures for both AC and AC–$FeCl_3$. It was also found that DMS was released over only one temperature interval centered at ~150 °C during the TPD process for sample AC–$FeCl_3$. This indicates that DMS that was desorbed at lower temperature in Fig. 6 was related to weak adsorption on the carbon phase and was almost been completely extracted by *n*-octane. In addition to DMS, DMDS and COS were also detected in the effluent gas from the

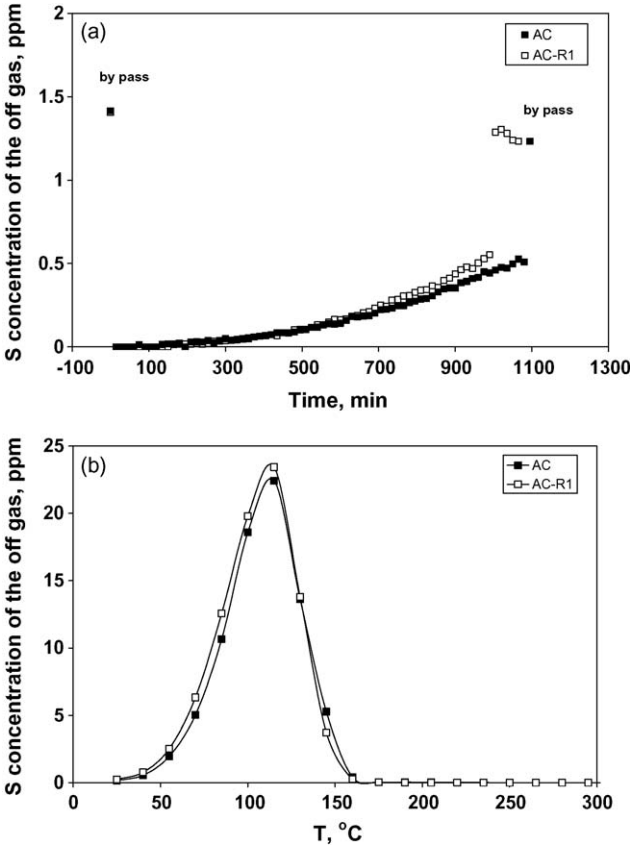

Fig. 8. Adsorption and desorption of sorbent AC and AC-R1. Sample AC-R1 had been used in a DMS breakthrough test with subsequent TPD regeneration prior to the current test.

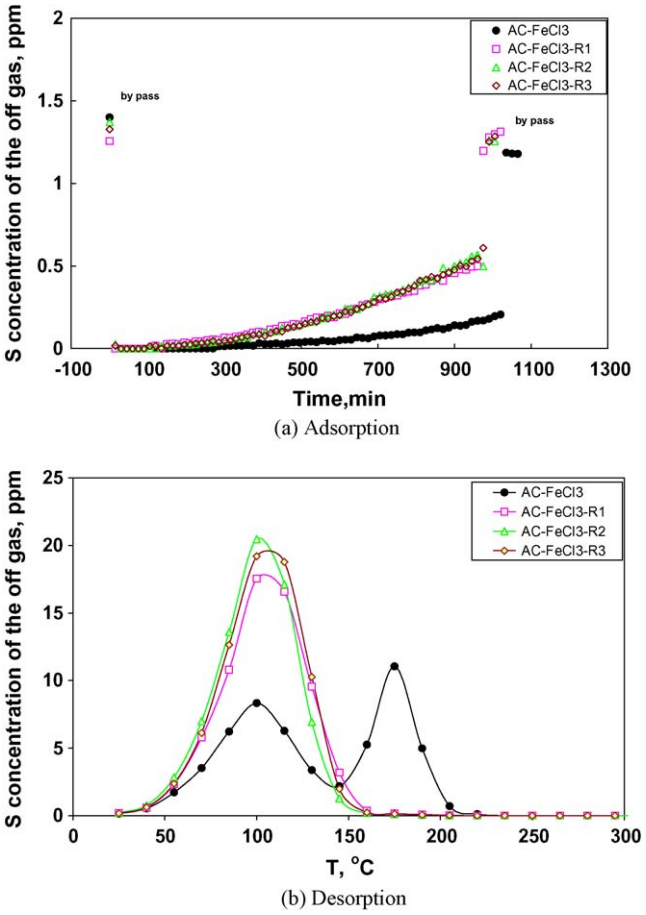

Fig. 9. Adsorption and desorption of fresh and regenerated AC–$FeCl_3$ sorbent samples. Regenerated samples are identified as AC–$FeCl_3$-R#, where # indicates the number of times the sample has been regenerated.

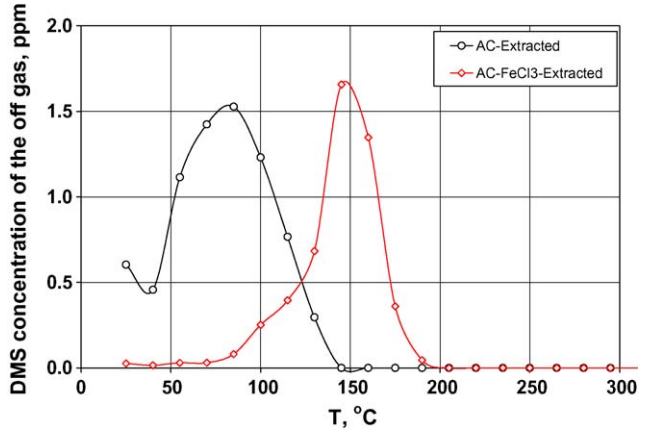

Fig. 10. Comparison of TPD curves of AC and AC–$FeCl_3$ samples that had been subjected to quantitative adsorption tests with DMS and then extracted with *n*-octane.

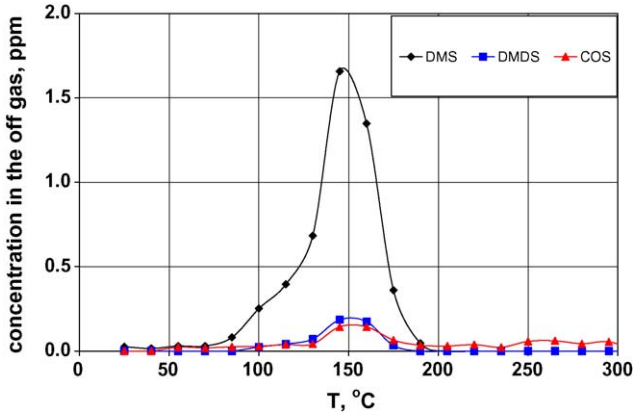

Fig. 11. TPD profiles of AC–$FeCl_3$ that had been subjected to a quantitative adsorption test with DMS and then extracted with *n*-octane.

Table 3
Sulfur recovery balance for AC and AC–$FeCl_3$ sorbents.

Sulfur distribution	AC	AC–$FeCl_3$
DMS loaded by adsorption milligram S per gram sorbent	0.389	0.412
DMS in n-octane extraction samples (liquid) milligram S per gram sorbent	0.213	0.161
Weight%	54.8	39.2
(DMS + COS + DMDS) recovered by TPD after extraction milligram S per gram sorbent	0.23	0.229
Weight%	57.8	55.7
Total S recovered as percentage of S loaded Weight%	112.6	94.9

thermal desorption of the AC–$FeCl_3$ sample that had been extracted, as shown in Fig. 11. This validates the findings of the TPD performed with the non-extracted samples and indicates that $FeCl_3$ plays a catalytic role in the formation of DMDS and COS during the thermal desorption.

Quantitative adsorption tests were intentionally conducted with similar sulfur mass loading. In the ideal case, all sulfur loaded on the samples during an adsorption test is expected to be recovered by solvent extraction or thermal desorption. Due to the small sorbent sample sizes, it was not possible to quantitatively analyze the sulfur content of the solid phase (i.e. sulfur that was not desorbed) after extraction and desorption to fully calculate a sulfur balance. Table 3 summarizes the distribution of sulfur recovered from the solid samples by *n*-octane extraction and thermal desorption. The total recovered as a percentage of the S loaded as DMS was 113% for virgin carbon AC and 95% for AC–$FeCl_3$. The sulfur distribution is almost the same for both sorbents, with nearly half extracted by *n*-octane and the other half released during TPD.

4. Conclusion

Activated carbon modified with $FeCl_3$ solution was shown to have an improved adsorption capacity for dimethylsulfide compared to the parent activated carbon, despite a notable decrease in the surface area and micropore area and volume. It can be inferred that the significant factor in the improvement of DMS capacity results from the new chemical properties created by the modification of $FeCl_3$ on the carbon surface rather than changes in the physical properties such as pore surface area and pore structure of carbon phase.

Samples with adsorbed DMS were extracted with *n*-octane and the resulting solvents were analyzed for sulfur compounds. Only DMS was detected in the extracts, indicating that DMS occupied the carbon surface rather than its oxidized form. The DMS-adsorbed samples were also subjected to temperature programmed desorption. The TPD pattern represented different kinetics of DMS desorption process, which related to the carbon phase and the new active sites. The new active sites improved DMS adsorption capacity and likely had stronger affinity with DMS molecule, which presented a regeneration challenge for used carbon sorbents. Thermal desorption is not an applicable option for regeneration of spent AC–$FeCl_3$. Thermal desorption cannot completely recover the original capacity due to the unstable thermal properties of the active sites created by $FeCl_3$. Thus alternative regeneration techniques should be investigated for industrial applications in the future.

Acknowledgements

This work was supported by the Office of Naval Research with contract number N00014-06-1-0086.

References

[1] Dimethyl Sulfide Overview, Gaylord Chemical Corporation, June 2007.
[2] M.C. Iliuta, F. Larachi, Journal of Chemical & Engineering Data 52 (1) (2007) 2–19.
[3] S. Satokawa, Y. Kobayashi, H. Fujiki, Applied Catalysis, B: Environmental 56 (1–2) (2005) 51–56.
[4] K. Takatsu, G. Takegoshi, H. Katsuno, Y. Kawashima, H. Matsumoto, Journal of the Japan Petroleum Institute 50 (4) (2007) 200–207.
[5] G. Alptekin, S. DeVoss, M. Dubovik, J. Monroe, R. Amalfitano, G. Israelson, Journal of Materials Engineering and Performance 15 (4) (2006) 433–438.
[6] A. Bagreev, J.A. Menendez, I. Dukhno, Y. Tarasenko, T.J. Bandosz, Carbon 43 (1) (2004) 208–210.
[7] T.J. Bandosz, Journal of Colloid and Interface Science 246 (1) (2002) 1–20.
[8] S. Bashkova, A. Bagreev, T.J. Bandosz, Environmental Science and Technology 36 (12) (2002) 2777–2782.
[9] I. Bezverkhyy, K. Bouguessa, C. Geantet, M. Vrinat, Applied Catalysis, B: Environmental 62 (3–4) (2006) 299–305.
[10] J. Guo, Y. Luo, A.C. Lua, R.-a. Chi, Y.-l. Chen, X.-t. Bao, S.-x. Xiang, Carbon 45 (2) (2007) 330–336.
[11] H. Hagio, Y. Fukagawa, Journal of the Japan Petroleum Institute 49 (2) (2006) 98–101.
[12] G. Israelson, Journal of Materials Engineering and Performance 13 (3) (2004) 282–286.
[13] J. Kim Dae, E. Yie Jae, Role of copper chloride on the surface of activated carbon in adsorption of methyl mercaptan, Journal of Colloid And Interface Science 283 (2) (2005) 311–315.
[14] H. Tamai, H. Nagoya, T. Shiono, Journal of Colloid and Interface Science 300 (2) (2006) 814–817.
[15] R. Yan, T. Chin, Y.L. Ng, H. Duan, D.T. Liang, J.H. Tay, Environmental Science and Technology 38 (1) (2004) 316–323.
[16] R.T. Yang, A.J. Hernandez-Maldonado, F.H. Yang, Science (Washington, DC, United States) 301 (5629) (2003) 79–81.
[17] H. Cui, M.A. Reese, S.Q. Turn, Abstracts of Papers 234th ACS National Meeting, Boston, MA, United States, August 19–23, 2007, FUEL-221.
[18] H. Cui, S.Q. Turn, M.A. Reese, Catalysis Today 139 (4) (2009) 274–279.
[19] S. Bashkova, A. Bagreev, T.J. Bandosz, Catalysis Today 99 (3–4) (2005) 323–328.
[20] H. Cui, S.Q. Turn, M.A. Reese, Energy & Fuels 22 (4) (2008) 2550–2558.
[21] A. Bagreev, S. Bashkova, T.J. Bandosz, Langmuir 18 (22) (2002) 8553–8559.